Electronic Supplementary Material (ESI) for ChemComm.

Supporting Information

Unprecedented superstructure in the Type I family of Clathrates

Philip Yox[a,b], Oleg Lebedev[c], Davide Donadio[d], Kirill Kovnir[a,b,*]

[a] *Department of Chemistry, Iowa State University, Ames, IA 50011, United States.*

[b] *Ames Laboratory, U.S. Department of Energy, Ames, IA 50011, United States.*

[c] *Laboratoire CRISMAT, ENSICAEN, CNRS UMR 6508, 6 Boulevard du Maréchal Juin, F-14050 Caen, France.*

[d] *University of California, Davis, Davis, CA 95616, United States.*

*Corresponding author: kovnir@iastate.edu

EXPERIMENTAL

Synthesis. *WARNING: Using large amounts of As inside sealed containers and heating to high temperatures can lead to explosion of the ampoule and release of toxic gases. For safety, all reactions were carried out in furnaces placed inside fume hoods with good ventilation, small amounts of As (< 200 mg) were used, and the temperature was ramped slowly.*
Starting materials used were Ba dendrites (Sigma Aldrich, 99.9%), Au powder (Alfa Aesar, 99.9%), and As lumps (Alfa Aesar, 99.999%). For crystal growth a 50/50 molar combination of CsI (Alfa Aesar 99.99%) and CsBr (Alfa Aesar 99.99%) were used. Arsenic was ground into a fine powder while the other elements were used as received. Carbonized, fused -silica ampoules (9 mm inner diameter, 11 mm outer diameter) were loaded inside of an Ar filled glovebox (O_2 < 0.5ppm) and subsequently evacuated and flame sealed.
Synthesis "From Elements" : Barium, gold, and arsenic were loaded into the carbonized, fused-silica ampoules in the stoichiometric ratio of 8 Ba, 16 Au, and 30 As. The ampoule was evacuated and flame-sealed, then placed in a muffle furnace and ramped to 600°C over 10 hours and annealed at 600°C for 120 hours. The furnace was allowed to cool naturally. The sample was opened in the glovebox, ground into a fine powder with an agate mortar and pestle, then reloaded in another ampoule and reannealed using the same furnace profile as the first annealing.
"Salt-Flux method" : Barium, gold, and arsenic were loaded into the carbonized, fused-silica ampoules in the ratio of 8 Ba, 16 Au, and 40 As. The total amount of Ba, Au, and As was 250 mg. 500 mg of a 50/50 molar combination of CsI and CsBr was added to the ampoule. The ampoule was evacuated and flame-sealed, then placed in a muffle furnace and ramped to 600°C over 10 hours and annealed at 600°C for 120 hours. The furnace was allowed to cool naturally. The ampoule was opened on air and the sample was washed with water to reveal block-like crystals with a metallic color.

Scanning Electron Microscopy/Energy Dispersive Spectroscopy (SEM/EDS)
Elemental analysis of samples was conducted using a FEI Quanta 250 field emission-SEM with EDS detector (Oxford X-Max 80, ThermoFischer Scientific, Inc., USA) and analyzed using the Aztec software. EDS show presence of only Ba, Au, and As in the sample synthesized from elements.

Single Crystal X-ray Diffraction. X-ray diffraction on a single crystal was performed using a Bruker D8 Venture diffractometer (Mo-K_α radiation). Datasets were collected at 100 K with φ- and ω-scans recorded at a 0.3° step and integrated using the Bruker SAINT software package. Multi-scan absorption correction was used. Structure solution and subsequent refinement was carried out with the SHELX suite.[1]

Powder X-ray Diffraction (PXRD). Laboratory PXRD experiments intended for phase identification were preformed using a Rigaku Miniflex 600 (Cu-K_α radiation with Ni-K_β filter). High-resolution synchrotron PXRD datasets were collected from beamline 11-BM at the Advanced Photon Source at Argonne National Lab (APS ANL). A Kapton capillary was loaded with $Ba_8Au_{16}As_{30}$ diluted with SiO_2. Rietveld refinements were performed with GSAS-II. A wavelength of 0.457910 Å was employed.

Transmission Electron Microscopy. High-resolution TEM (HRTEM) and electron diffraction (ED) studies were performed using a Tecnai G2 30 UT (LaB_6) microscope operated at 300 kV with 0.17 nm point resolution and equipped with an EDAX EDX detector. High angle annular dark field (HAADF)–scanning TEM (STEM) and annular bright field scanning TEM (ABF-STEM) studies were performed using a JEM ARM200F cold FEG double aberration corrected electron microscope operated at 200 kV and equipped with a large solid-angle CENTURIO EDX detector and Quantum EELS spectrometer.

Sample Densification. Dense pellets were prepared using spark plasma sintering (Dr. Sinter Lab Jr. 211 Lx). $Ba_8Au_{16}As_{30}$ was finely ground in an agate mortar and pestle before being loaded into a 5 mm graphite die with tungsten carbide plungers. 51 MPa of uniaxial pressure was applied while the temperature was ramped to 523 K over 7 minutes. Once the temperature reached 523 K, 153 MPa was applied and held for 10 minutes. After, pressure was abruptly released to prevent any cracking upon cooling. The Archimedes method was used to determine that the pellet had 91% of the theoretical density determined from single crystal X-ray diffraction. PXRD confirmed that no decomposition had occurred during densification.

Transport Properties. Thermal conductivity and Seebeck coefficient were measured from 10 K to 300 K on a 5 mm diameter polycrystalline pellet using the Thermal Transport option on the Quantum Design PPMS Evercool II. Electrical resistivity was measured from 2 K to 300 K on a cut bar from the same 5 mm pellet using a four-probe geometry with the Resistivity option on the PPMS Evercool II.

DFT Calculations. We have computed the relaxed structure and the equation of state of $Ba_8Au_{16}As_{30}$ by density functional theory in generalized gradient approximation using the functional Perdew, Burke and Ernzerhof (PBE)[2] in the plane-waves pseudopotential formalism.[3] The plane waves basis set for the Kohn-Sham orbitals is truncated at a cutoff of 40 Ry, and Projector Augmented Wave pseudopotentials[4] are used to treat nuclei and core electrons. The electronic structure is integrated on a 4x4x6 uniform grid of *k*-points. To address the shortcomings of local density and GGA functionals in describing the electronic structure of correlated systems, we apply a Hubbard (GGA+U) correction to the *d*-orbitals of Au ($U = 5\ eV$) and the *p*-orbitals of As ($U = 3\ eV$).[5] Besides improving the band structure, the GGA+U approach provides a better estimate of the equilibrium volume of the system (Table S3).

Electronic transport coefficients are computed using the semiclassical Boltzmann transport equation in the relaxation time approximation, as implemented in the BoltzTrap code.[6] For these calculations, the GGA+U Kohn-Sham bands are integrated over a uniform 8x8x12 grid of *k*-points.

Table S1. Single crystal data and refinement parameters for $Ba_8Au_{16}As_{30}$.

$Ba_8Au_{16}As_{30}$			
	Single Crystal	Powder Diffraction	DFT
Temperature (K)	100	295	
Radiation (Å)	Mo-K_α, 0.71073	0.457910	
Crystal System	Monoclinic		
Space group	$P2_1/c$ (No. 14)		
a (Å)	15.147(1)	15.19733(3)	15.310
b (Å)	15.218(1)	15.26112(3)	15.389
c (Å)	10.954(1)	10.97885(2)	11.073
β (degrees)	90.502(2)	90.4443(2)	90.45
Volume (Å^3)	2525.1(4)	2546.229(6)	
Z	2		
Data/parameters	6719/248		
Density (g·cm^3)	8.546		
μ (mm^{-1})	71.902		
R_{int}	0.090		
G-o-F	1.06		
R_1 [$I > 2\sigma(I)$]	0.032		
wR_2 [$I > 2\sigma(I)$]	0.054		
R_1 [all data]	0.050		
wR_2 [all data]	0.058		
Diff. peaks [e·Å^{-3}]	2.18/-2.36		

Further details of the crystal structure investigations may be obtained from the joint CCDC/FIZ Karlsruhe online deposition service: https://www.ccdc.cam.ac.uk/structures/? by quoting the CSD deposition number 2109533.

Table S2. Cage volumes, average and shortest bond distances to Ba for $Ba_8Au_{16}As_{30}$ and $Ba_8Au_{16}P_{30}$

	$Ba_8Au_{16}P_{30}$	$Ba_8Au_{16}As_{30}$	Relative increase, $(\frac{As-P}{P})$
5^{12} Cage Volume (Å^3)	112.67	128.08	13.7 %
$5^{12}6^2$ Cage Volume (Å^3)	154.19	175.89	14.1 %
5^{12} Cage Avg. Bond (Å)	3.41	3.55	4.3 %
$5^{12}6^2$ Cage Avg. Bond (Å)	3.73	3.88	4.1 %
5^{12} Cage Short Ba-Pn distance (Å)	3.33	3.45	3.6 %
$5^{12}6^2$ Cage Short Ba-Pn distance (Å)	3.38	3.57	5.6 %
5^{12} Cage Short Ba-Au distance (Å)	3.30	3.39	2.7 %
$5^{12}6^2$ Cage Short Ba-Au distance (Å)	3.42	3.53	3.2 %

Table S2.2 Cage volumes, average and shortest bond distances to Ba for experimental $Ba_8Au_{16}As_{30}$ ($P2_1/c$) and hypothetical orthorhombic unrelaxed structure of $Ba_8Au_{16}As_{30}$ (*Pbcn*). This provides the direct comparison of volumes and distances, as the per formula unit volume is held to be the same.

	$Ba_8Au_{16}As_{30}$ ($P2_1/c$)	$Ba_8Au_{16}As_{30}$ (*Pbcn*)	Relative increase, $\frac{Pbcn - P2_1/c}{P2_1/c}$
5^{12} Cage Volume (Å^3)	128.08	128.31	0.2 %
$5^{12}6^2$ Cage Volume (Å^3)	175.89	175.58	-0.2 %
5^{12} Cage Avg. Bond (Å)	3.55	3.55	0 %
$5^{12}6^2$ Cage Avg. Bond (Å)	3.88	3.88	0 %
5^{12} Cage Short Ba-Pn distance (Å)	3.45	3.45	0 %
$5^{12}6^2$ Cage Short Ba-Pn distance (Å)	3.57	3.51	-1.7 %
5^{12} Cage Short Ba-Au distance (Å)	3.39	3.47	2.4 %
$5^{12}6^2$ Cage Short Ba-Au distance (Å)	3.53	3.61	2.3 %

Table S3. Computed lattice parameters and Bulk modulus of $Ba_8Au_{16}As_{30}$ ($P2_1/c$) from DFT GGA and GGA+U.

	GGA(PBE)	GGA+U
a (Å)	15.504	15.310
b (Å)	15.569	15.389
c (Å)	11.200	11.073
β (degrees)	90.50	90.45
Density (g/cm^3)	7.98	8.27
B (GPa)	60.4	68.8

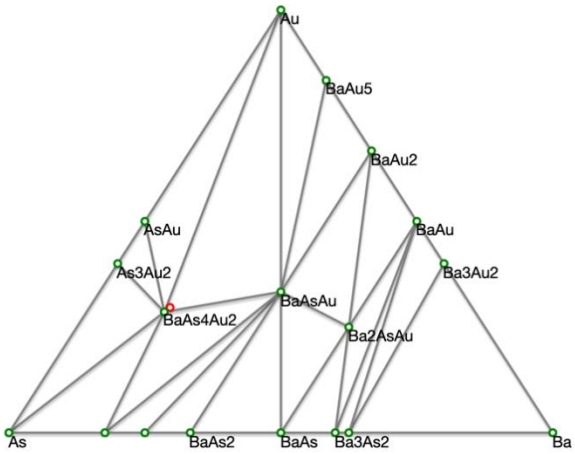

Figure S1. Ternary phase diagram of Ba-Au-As system. $Ba_8Au_{16}As_{30}$ (red) is slightly less stable than the compositionally similar hypothetical phase $BaAu_2As_4$, according to the shown triangle with a decomposition energy $\Delta E = 0.016\ eV/atom$: $3Ba_8Au_{16}As_{30} \rightarrow 22BaAu_2As_4 + 2Au + 2BaAuAs$. The formation energy of $Ba_8Au_{16}As_{30}$ is $\Delta E_f = E_{Ba8Au16As30} - 8E_{Ba}(s) - 16E_{Au}(s) - 30E_{As}(s) = -0.429$ eV/atom. These energies are computed at the level of GGA without +U corrections.

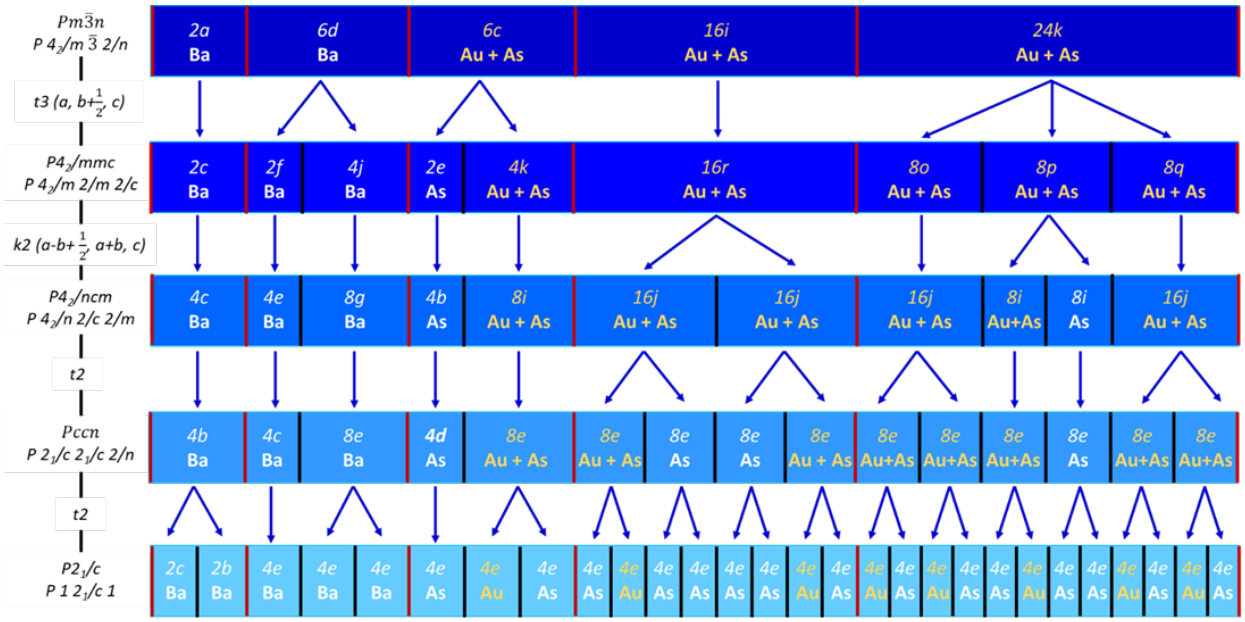

Figure S2. Bärnighausen tree showing the Wyckoff site splitting from aristotype *Pm*$\bar{3}$*n* to hettotype *P*2$_1$/*c*. In this tree, only in *P*2$_1$/*c* the mixed occupancy of all Wyckoff sites can be avoided. The program WYCKSPLIT[7] was utilized.

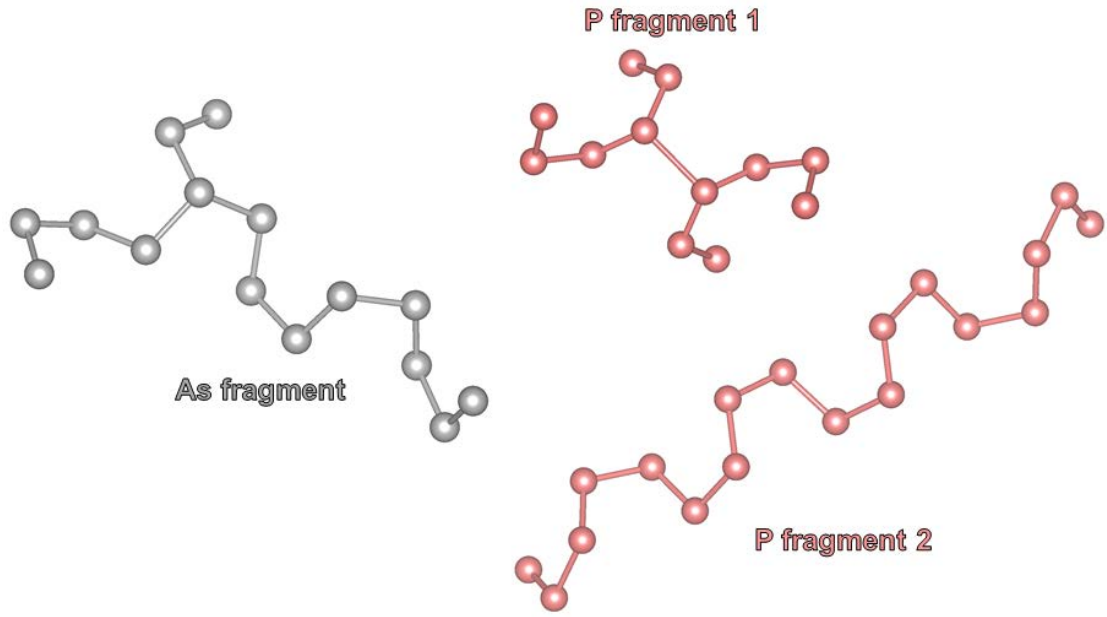

Figure S3. $Ba_8Au_{16}As_{30}$ exhibits only one kind of As fragment composed of 15 arsenic atoms. $Ba_8Au_{16}P_{30}$ exhibits two kinds of P fragments with one 12 member branched fragment featuring a long (2.72 Å) P-P bond in the middle, the second P fragment is a helical chain of 18 P atoms.

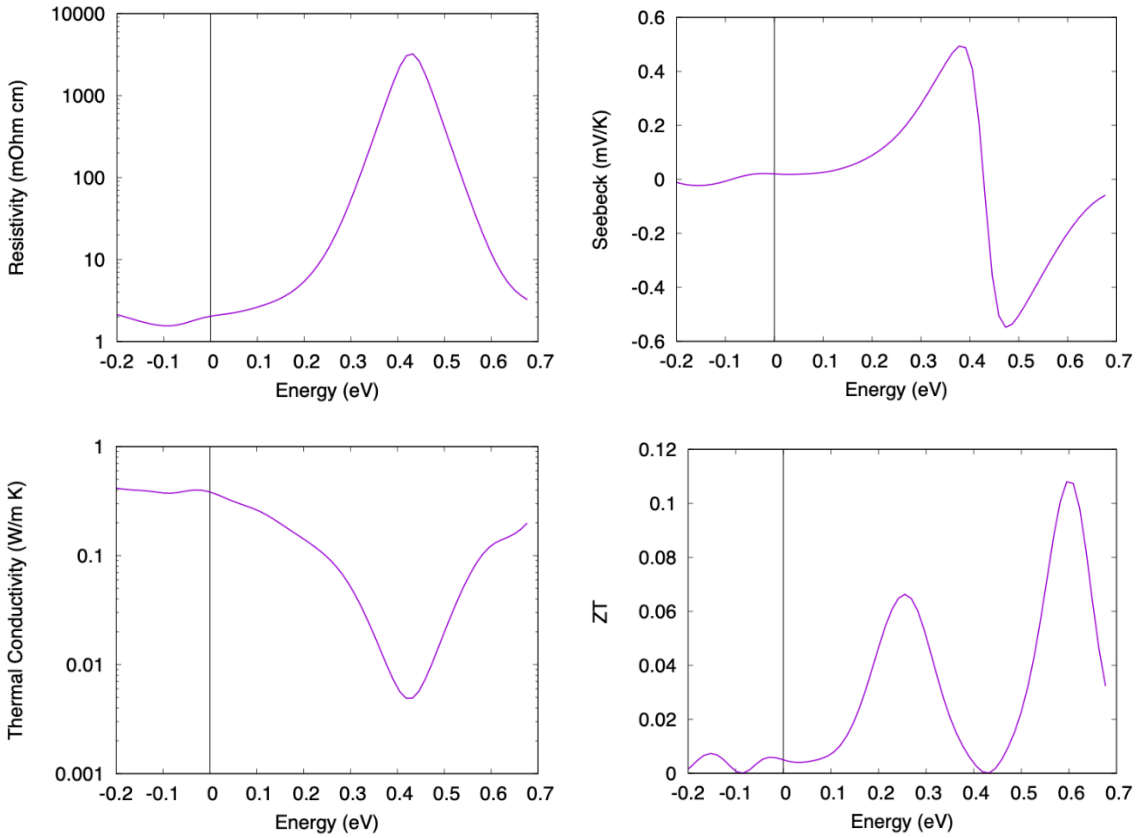

Figure S4. Transport coefficients of $Ba_8Au_{16}As_{30}$ ($P2_1/c$) as a function of the shift of the Fermi energy: electrical resistivity, Seebeck coefficient, electrical contribution to the thermal conductivity and figure of merit ZT, computed by GGA+U and the semiclassical Boltzmann transport equation. In these calculations we use a fine grid of k-points (8x8x12) and we assume a relaxation time of $\tau = 5\ fs$. This choice is arbitrary, but it gives the electrical resistivity and electronic contribution to the thermal conductivity in the same ballpark as the measurements. We use the measured value $\kappa_{ph} = 0.85\ Wm^{-1}K^{-1}$ as lattice thermal conductivity to estimate ZT. The undoped material is a p-type degenerate semiconductor. Shifting the Fermi level would enhance ZT significantly, but not beyond 0.1.

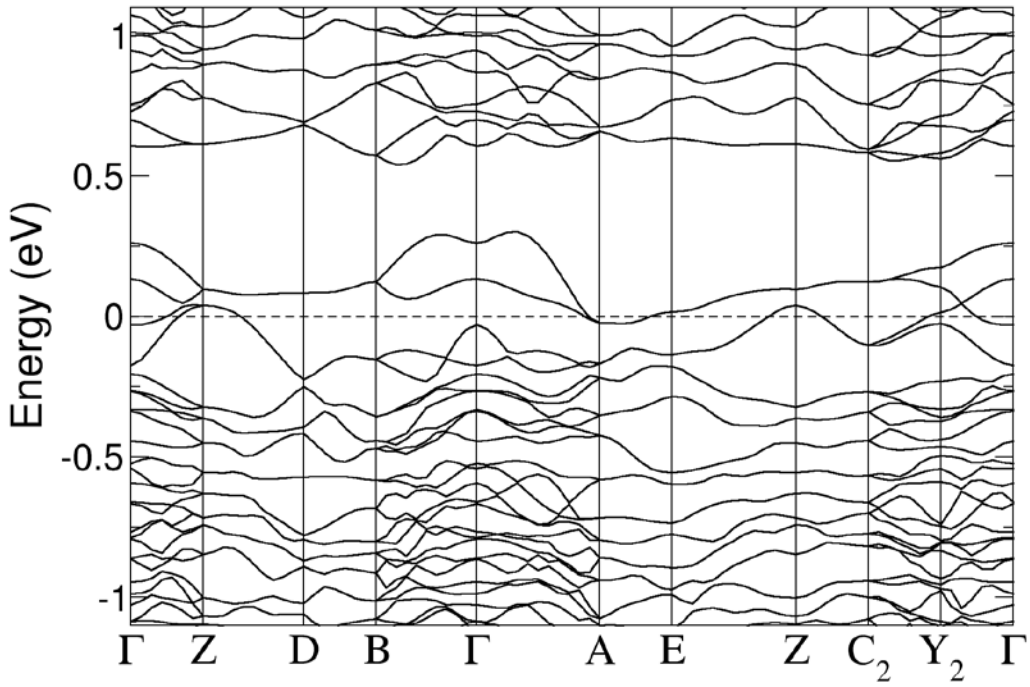

Figure S5. Band structure of $Ba_8Au_{16}As_{30}$ ($P2_1/c$) computed by density functional theory in the generalized gradient approximation with Hubbard corrections (GGA+U).

REFERENCES

1. G. M. Sheldrick, Acta Crystallogr. A, 2008, **64**, 112–122
2. J. P. Perdew, K. Burke and M. Ernzerhof, Phys. Rev. Lett., 1996, **77**, 3865–3868.
3. 1P. Giannozzi, O. Andreussi, T. Brumme, O. Bunau, M. Buongiorno Nardelli, M. Calandra, R. Car, C. Cavazzoni, D. Ceresoli, M. Cococcioni, N. Colonna, I. Carnimeo, A. Dal Corso, S. De Gironcoli, P. Delugas, R. A. Distasio, A. Ferretti, A. Floris, G. Fratesi, G. Fugallo, R. Gebauer, U. Gerstmann, F. Giustino, T. Gorni, J. Jia, M. Kawamura, H.-Y. Ko, A. Kokalj, E. Küçükbenli, M. Lazzeri, M. Marsili, N. Marzari, F. Mauri, N. L. Nguyen, H.-V. Nguyen, A. Otero-De-La-Roza, L. Paulatto, S. Poncé, D. Rocca, R. Sabatini, B. Santra, M. Schlipf, A. P. Seitsonen, A. Smogunov, I. Timrov, T. Thonhauser, P. Umari, N. Vast, X. Wu and S. Baroni, J. Phys. Condens. Matter, 2017, **29**, 465901.
4. Blöchl, P. E. Projector augmented-wave method. *Phys. Rev. B*., 1994, **50**, 17953–17979.
5. B. Himmetoglu, R. M. Wentzcovitch and M. Cococcioni, *Phys. Rev. B*, 2011, **84,** 115108.
6. G. K. H. Madsen and D. J. Singh, *Comput. Phys. Commun.*, 2006, **175**, 67–71.
7. E. Kroumova, J. M. Perez-Mato and M. I. Aroyo, *J. Appl. Cryst.*, 1998, **31**, 646.